

Article Title: Green Synthesis of Cobalt Doped Nickle Ferrite Nanoparticles via Extract of Vitis Vinifera and its impact on Structural, Optical and Magnetic Properties

Bibi Zahida¹, Jafar Khan Kasi¹, Ahmed Bilal¹, Shehzad Ahmed¹, Syed Wajahat Ali¹, Ajab Khan Kasi¹

¹Department of Physics, University of Balochistan, Quetta, Pakistan.

Corresponding Email: zbibi6@gmail.com

Received: 07 March 2024 Published: 24 July 2024

Abstract:

This research highlights the significance of an environmentally safe green synthesis method for achieving magnetic nanoparticles, and the impact of Co doping on Nickle ferrites. Three samples, NiFe₂O₄, Ni_{0.7}Co_{0.3}Fe₂O₄ and Ni_{0.5}Co_{0.5}Fe₂O₄ were prepared by using the extract of Vitis vinifera (black raisins) as reducing agent/ fuel followed by the sol-gel auto combustion method. This study also examines the effect of pH on the optimum yield of NPs. various characterization techniques were performed to determine the morphological, optical and magnetic properties of prepared samples. XRD characterization verified the single-phase FCC crystalline structure of the samples, and the average crystallite sizes for the formed NPs were found to be 16.8 nm, 17.5 nm and 18.9 nm respectively. The EDX analysis verified the anticipated elemental composition of all the samples. FTIR analysis confirmed the presence of phenolic contents in the samples. The Optical band gaps for the samples were determined by UV-vis spectroscopy and recorded as 2.92 eV, 3.48 eV and 3.4 eV respectively. SEM analysis was performed to confirm the shape, structure, and the particle sizes of the samples. The average particle sizes were recorded as 46 nm, 57 nm, and 68 nm for NF, CNF1 and CNF2. Magnetic properties of all the samples were analyzed via VSM characterization. The ferromagnetic properties were found to be enhanced by Co doping, as the dopant increases the saturation magnetization increased from 29.6 emu/g to 30.2 emu/g and 37.8 emu/g respectively, further the remnant magnetization was also increased from 3.01 emu/g to 4.5 emu/g and 5.7 emu/g. hence, molding the properties of CNF to make it preferable for various applications.

Keywords: Vitis vinifera, green synthesis, Co doping, Nickel Ferrite, Nanoparticles.

DOI Number: <https://10.52700/jn.v5i2.103>

© 2024 The authors. Published by The Women University Multan. This is an open access article under the Creative Commons Attributions-NonCommercial 4.0.

Introduction

In this modern era of research and technology where humans are solving complex problems on atomic and subatomic levels and addressing global challenges. Nanotechnology is one of the most crucial and universal problem solvers. It has taken a lead over all other technologies in every walk of life i.e., medical, cosmetics, sanitation and industries etc. [1].

Currently, much of the research is conducted on nano particles and their various applications. Because of their tremendous properties and uses, it has become one of the most fascinating fields for researchers worldwide [2-3] on a nano scale the properties, color and size of every element is transformed into a new object with molded properties. There are various types of nanomaterials having various applications i.e., carbon-based nanomaterials, metal-based nanomaterials, dendrimers and polymeric nano materials/ particles [4]. All these particles have their own properties and characteristics based on which they are used in various technologies/ applications.

Among all the nano materials magnetic nano particles (MNPs) are one of the most popular materials because of their excellent properties in almost all emerging applications of the present world. Magnetic nano particles are used to treat fetal diseases such as cancer, used as magnetic recording media, used for removing the venomous particles from the water, used as a dyeing material for various things etc. hence it has become a part of every solution almost in every walk of life [3, 5, and 6]. Its countless beneficial properties and applications have made it an eye-catching field for the whole globe. MNPs contain spinel structures that can be normal spinel structure, inverse or mixed spinel structures [7]. Nickel and cobalt ferrites possessing spinel structure (the magnetic nanomaterials), with highly special properties making them special magnetic materials that are widely used in so many applications. [2, 6], Ni ferrites are found with normal and inverse spinel structure possessing formula AB_2O_4 , in normal spinel structure A (divalent metal cations, i.e. Cu, Co, Ni, Mg, Mn, Zn etc) occupy tetrahedral sites and B are the trivalent (Fe^{+3}) cations distributed between octahedral and tetrahedral sites, whereas in inverse spinel structure the divalent cations contain octahedral sites and the trivalent cations occupy the tetrahedral and octahedral sites respectively [7-8]. A spinel ferrite is of FCC form containing 08 units and each unit comprises 64 tetrahedral sites A, and 32 octahedral sites B [9-10].

The Ni ferrites ($NiFe_2O_4$) undergo very good electrical and electrochemical properties; they can withstand high resistances and possess low eddy current losses. Therefore, these ferrites can be used as a high-density storage device, microwave absorbers, antennas, as sensors, and

are able to produce hyperthermia to destroy and treat cancerous cells and as a drug delivery agent to various cells where needed [11]. Ni ferrites can also be applied as anti-bacterial agents and can be used to remove the heavy metals i.e. Cr, Cd, and Pb etc from water or other wastes to recycle them. [12]. they are also used in MRIs and as immunoassays etc [13]. Whereas Co ferrites (CoFe_2O_4) containing an inverse spinel structure, also possess many tremendous and relating applications i.e. they are used as energy storage devices, capacitors, biomedical uses, antibacterial agents etc. [14]. Nickel ferrites belong to soft magnetic material amid all other magnetic materials/ ferrites, being a soft magnetic material, it has higher magnetic saturation, and higher resistivity due to which it possesses less eddy losses. It has also the quality of lower coercivity and lower retentively [15]. To enhance or modify its properties i.e. increasing its magnetization saturation, structural properties, and chemical stability, and size etc. the nickel ferrites can be doped with other divalent, trivalent or tetravalent materials as per requirement. So, choosing an appropriate metal cation for doping is one of the most important aspects as per requirement of application [16]. The divalent dopants are mostly Cu, Co, Ni, Mg, Mn, Zn etc. one of the crucial dopants because of its tremendous properties is cobalt possessing inverse spinel structure and belongs to hard magnetic materials hence doping it with Ni ferrites enhances its magneto-crystalline anisotropy (saturation magnetization, remnant magnetization and coercivity) [11, 17]. Another important aspect of cobalt is its larger radii as compared to Ni, when doped with the Ni molds the parameters of the formed ferrites such as lattice size, cationic distribution, structure, magnetic properties and grain size respectively [2, 18-19] Cobalt doped nickel ferrites are also soft ferromagnetic materials with enhanced properties, having FCC lattice structure, it contain binding properties hence, can be used as electromagnetic shielding, magnetic recording media and as adsorbents for heavy metals from water [20]. The cobalt doped nickel ferrites have also been used extensively as antibacterial agents for the treatment of cancer through inhibition of PI3K/Akt/mTOR pathway [21]. These particles are used for treatment purposes such as magnetic resonance imaging (MRI) mostly used for internal imaging of the human body, it's also used for drug delivery system to the effected cells within the body, in medical field it's also being used as anti-microbial agent for various purposes [22]. Possessing marvelous magnetic properties, these materials are preferred in all magnetic devices such as, permanent magnets, are highly used in magnetic tapes, almost in all radio frequency circuits and high-quality filters, these are used in recent wave guided isolators, also as high frequency inductors, they are used as gas sensors, they are also used as microwave absorbers and super capacitors [23]. By doing Ni with Co increases coercivity of the particles therefore

gaining better remnant magnetization and saturation magnetization, hence increasing the magnetic properties of Ni ferrites [24].

Magnetic nano particles can be synthesized via various methods i.e., chemical methods (chemical reduction, sol-gel, hydrothermal, micro emulsion, co-precipitation etc.) [10- 12, 17, 25], physical methods (sputtering, laser ablation, ball milling, thermal evaporation etc.) [26], and green synthesis methods. Green synthesis method is one of the most preferable and easy methods that can lead to a clean environment, low cost and easy to manage. This method uses any available plant or any of its part as a fuel instead of harmful acids. Green synthesis followed by auto combustion method is one of the excellent and uncomplicated ways to prepare pure and single spinal phase nanoparticles with effective cost and producing less poisonous gases into the environment as compared to the other synthesis methods [2, 27]. The green method is mostly used method for forming MNPs and is extensively used in the recent era as they possess more advantages over the other methods. The phenols present in plants react with the metal salt ions to synthesize the MNPs [28]. pH and temperature optimization play a key role in the synthesis process of MNPs, pH acts as a catalyst in the synthesis of NPs, hence finding the proper pH and optimum temperature for the maximum speed and high yield of NPs for any green synthesis process is a crucial step [2, 29]. For the green synthesis process of NiFe₂O₄ and Co doped NiFe₂O₄ many plants (leaves, seeds, flowers, roots etc.) have been used so, far for cobalt doped Ni ferrites synthesis the green fuels used are Corian drum sativum plant extract [21], Aloe Vera extract [30], and Andrographis paniculata extract [31].

This study is performed to determine various properties for Ni and Co doped Ni ferrites via green synthesis. In this study Vitis vinifera extract (that has not been used before) is used as a capping agent to greenly synthesize NFs (nickel ferrites), CNFs (cobalt doped nickel ferrites), and the impact of Co doping on Ni is studied in detail. The comparison between the two is investigated by performing various characterizations through standard tools.

Experimental Methods

Chemicals used

The chemicals used were Folin Ciocalteu, DI water, analytical grade Nickel nitrate salt Ni(NO₃)₂.6H₂O, of 99% purity, cobalt nitrate Co(NO₃)₂.6H₂O of 99% purity and Iron nitrate Fe(NO₃)₂.6H₂O, of 99% purity, sodium carbonate (Na₂CO₃) sodium hydroxide (NaOH), Black raisins extract that was used as fuel.

Plant extraction process

Vitis vinifera (black raisins 100 grams) were taken, washed, dried and cut into small pieces. For extraction process 25 g of cut raisins were mixed in 100 ml of DI water, at the optimized temperature that was 60 °C for 20 minutes on hot plate magnetic stirrer. To remove impurities from the formed extract it was centrifuged and stored in refrigerator for further use.

Synthesis of NFs, CNF1 and CNF2 by green rout followed by auto-combustion

For the synthesis process of Nickel Ferrite (NF) Ni nitrate and iron nitrate salts were added in ratio 1:2 (1 g Ni and 2 g of Fe) into 40 ml of DI water and were stirred vigorously to get thoroughly dissolved. Then the extract of black raisins 25ml which acted as a fuel was added into the aqueous solution of salts and 0.16 g of NaOH solution which was prepared separately in DI water was added drop by drop into this solution until pH 9 was attained, and stirred for 30 minutes at 60 °C and later the temperature was increased to 100 °C and was left for evaporation of extra water and a gel like solution was formed and the initiation of auto-combustion process took place forming a brown color NPs, these NPs were collected and were thoroughly washed with DI water to remove the impurities and were centrifuged, this process was repeated twice to get pure NPs. Later these particles were poured into a china dish and were heated in furnace at 130°C to dry and improve its crystallinity, once heated these particles were collected and grinded as per requirement and stored in an airtight bag.

In order to synthesize the first doped sample (CNF1), the ratio of the salts remained the same i.e. 1:2 the iron nitrate remained the same i.e. 2 g and the Ni nitrate were divided as 0.3 g Co and 0.7 g Ni was mixed to form 1 g. The synthesis process was the same as mentioned for NF. Finally, for the synthesis process of second sample (CNF2) the Ni nitrate was divided as 0.5 g of Co and 0.5 g Ni were mixed to form 1g and the synthesis process was the same as used for the NF sample.

Characterization Methods

In order to investigate various properties of the formed NPs such as shape, size, phase, purity, morphology, topography, functional group, and magnetic properties etc the following characterizations were performed: XRD confirms crystal structure of the formed NPs, SEM confirms morphology and topography, UV-vis determines the energy band gaps, FTIR determines the vibrational modes and functional group, EDX confirms the expected elemental composition and VSM verifies the magnetic properties of the samples.

Results and Discussion

XRD results

To determine the phase and crystal structure of the synthesized NF, CNF1 and CNF2 XRD was performed. In an ideal case the synthesized NPs should be of a pure crystalline structure and should possess a single phase, which can be determined via various standard JPCDS card numbers indicating various peaks [32], the XRD results in addition provides other information about various parameters such as surface area, the chemical bonds, crystallite size, X-ray density etc.

The XRD results for all the samples were analyzed through Xpert highscore software. The XRD patterns for NF, CNF1 and CNF2 are shown in figure 1. The lattice peaks for NF were recorded (1 1 1), (2 2 0), (3 1 1), (2 2 2), (4 0 0), (3 3 1), (4 2 2) and (5 1 1) matching with the JCPDS card no. 01-074-1913, which has been reported in some other study as well [32], indicating the single phased pure fcc cubic structure of the crystals and no impurity peaks were observed. The lattice parameters denoted by a, b, and c for a cubic structure were calculated for the highest peaks from the formula

$$a = \frac{\lambda\sqrt{(h^2 + k^2 + l^2)}}{2\sin\theta} \quad (1)$$

Where λ is X-ray wavelength and its value in this case is equal to 1.5406\AA , h, k, and l are the miller indices and θ is the Bragg's angle. The value of "a" was recorded as 8.3580\AA OR 0.83580nm , which was same for other two side b and c, and was found to be matched with JCPDS card no. 10-0325, that also consistent with the result 0.8339nm [3].

The volume of the cell was calculated as 0.5631nm^3 by using formula

$$V = a^3\text{nm} \quad (2)$$

The crystal size was calculated by using Debye's Scherer equation using the highest peak (3 1 1)

$$D = K \lambda / \beta \cos\theta \quad (3)$$

Where D is the crystallite size, K is the correction factor for the shape of particles, and its value is 0.9. λ is X-ray wavelength, β is full width half maxima and θ is the Bragg's angle [33]. The size of the crystal for nickel ferrites was recorded as 16.8 nm . The value might be greater to some extent because of the micro strain that has not been calculated.

The X-ray density denoted by dx was calculated by using the formula:

$$dx = ZM/Na.a^3 \quad (4)$$

Where Z is the quantity unit formula weighing 8 and M is the molecular weight of Ni ferrite weighing 234.381 g/mol , Na is the Avogadro's number and its value is $6.02 \times 10^{23}/\text{mol}$ and a is the lattice constant. And the dx for NF was recorded as 5.53 g/cm^3 .

The surface area for NF was calculated as $64.58\text{ m}^2/\text{g}$ by using formula:

$$S.A = 6/dx. D \quad (5)$$

The dislocation density was calculated by using the formula:

$$\delta = 1/D^2 \quad (6)$$

The dislocation density for NF was recorded as 3.05 g/cm³.

The XRD peaks for CNF1 were recorded as (1 1 1), (2 2 0), (3 1 1), (2 2 2), (4 0 0), (3 3 1), and (4 2 2) matching JCPDS card no. 00-010-0325 which has also been reported somewhere else [24] the ferrites were found to be of fcc cubic structure belonging to space group Fd3m. The XRD peaks CNF2 were found as (1 1 1), (2 2 0), (3 1 1), (2 2 2), (4 0 0), (3 3 1), (4 2 2), and (5 1 1) matching with the JCPDS card no. 01-080-0072, having single phase cubic structure belonging to Fd3m space group. The lattice parameter, volume of nanoparticles and other related parameters for NF, CNF1 and CNF2 were calculated by using the above-mentioned formulae and are mentioned in the table 1 and 2.

From the results mentioned in table 1 and 2, a small shift is observed in 2θ with increasing Co concentration and the lattice parameter “a”, volume of the cell “V”, and inter planer distance “d” are also found to increase with an increase in the Co concentration. The crystal size is also increased by Co doping, whereas, the X-ray density, surface area and dislocation density are found to decrease as the concentration of the Co is increased, these results are in consistent with some other studies [1,2 and 34]

Table 1: comparison of lattice parameter and volume for NF, CNF1, and CNF2

Sample	hkl	λ (nm)	2θ (deg)	θ (deg)	θ (rad)	a(nm)	V (nm ³)	d (nm)
NF	311	0.1456	36.043	18.0215	0.31453	0.82580	563.15	2.48988
CNF1	311	0.1456	35.700	17.8500	0.31154	0.83390	579.89	2.51300
CNF2	311	0.1456	35.644	17.822	0.31105	0.83473	581.62	2.51681

Table 2: values of D, dx, S.A, and δ for NF, CNF1 and CNF2

Sample	Crystal size (nm)	X-ray density (g/cm ³)	Surface area (m ² /g)	Dislocation density 10 ¹⁵ (m ⁻²) δ
	D	dx	S.A	
NF	16.8	5.53	64.58	3.25
CNF1	17.5	5.37	62.66	3.06
CNF2	18.9	5.25	60.01	2.01

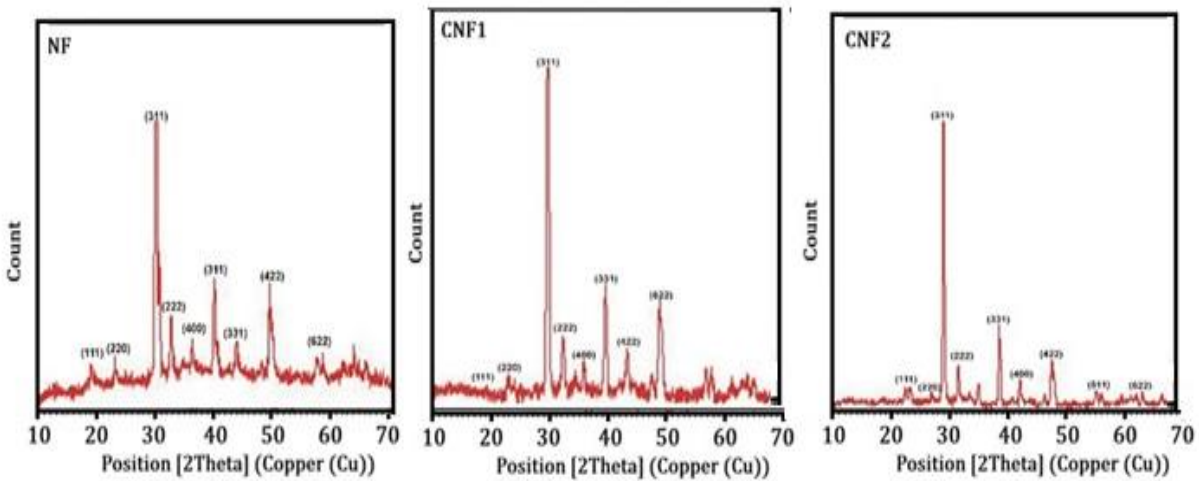


Fig. 1 XRD pattern of NF, CNF1 and CNF2

EDX analysis

Energy dispersive x-ray was carried out to verify the existence of anticipated elements on the formed NPs. The elemental peaks for NF, CNF1 and CNF2 are shown in the figure 2 and there are no impurity peaks seen in the figure. The values of wt % and atomic% for all the elements are given in table 3.

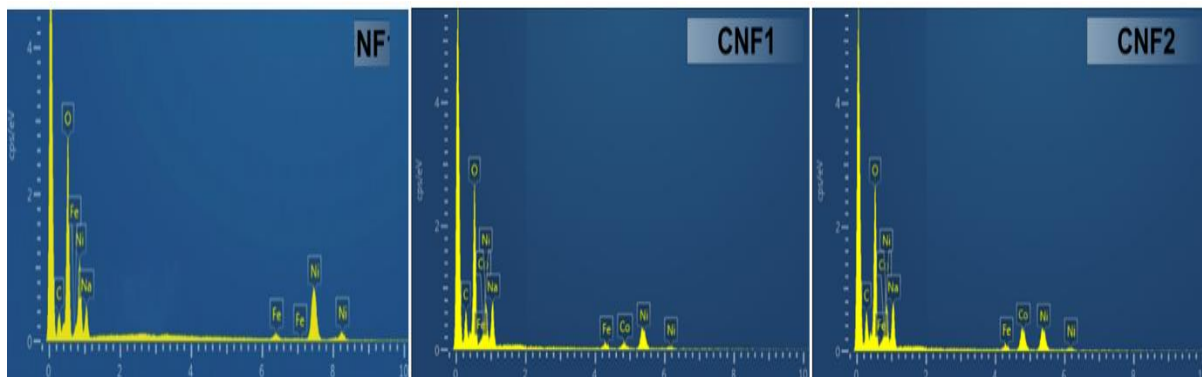


Fig. 2 EDX peaks of samples NF, CNF1 and CNF2

SEM analysis

This characterization was performed to investigate about morphology (the shape and structure), arrangement of atoms (topography) and grain size of the NPs. The SEM analysis was carried out by Nova 450 nano SEM at 200kx. The images for NF, CNF1 and CNF2 are shown in figure 3. Randomly 50 NPs of various sizes were selected for the average size

Table 3: The values of wt %, atomic% of Ni, Co, Fe and O present in NF, CNF1 and CNF2

Elements	NF		CNF1		CNF2	
	Weight %	Atomic %	Weight %	Atomic %	Weight %	Atomic %
Ni	23.8	13.67	15.23	10.49	10.32	7.99
Co	Nil	Nil	13.44	9.65	8.21	5.77
Fe	46.3	29.31	45.72	27.78	40.37	21.60
O	26.66	55.25	20.13	46.24	18.97	39.56

calculation of NPs and the calculated average sizes were recorded as 46 nm, 57 nm and 68 nm for NF, CNF1 and CNF2 respectively. The images for NF, CNF1 and CNF2 are shown in figure 3. Randomly 50 NPs of various sizes were selected for the average size calculation of NPs and the calculated average sizes were recorded as 46 nm, 57 nm and 68 nm for NF, CNF1 and CNF2 respectively. Some particles were formed to be dense and in agglomerated form i.e. 300 nm indicating the magnetic behavior of NPs, while the other reason for the formed agglomerations could be the removal of phenols present on the plant extract acting as balancing agents that avoids the particles from forming agglomerations [35], the synthesized particles are found to be of spherical shapes, some in cylindrical, oval and some in irregular shapes as shown in figure 3. The particle size is found to increase with Co doping which is consistent with the XRD results.

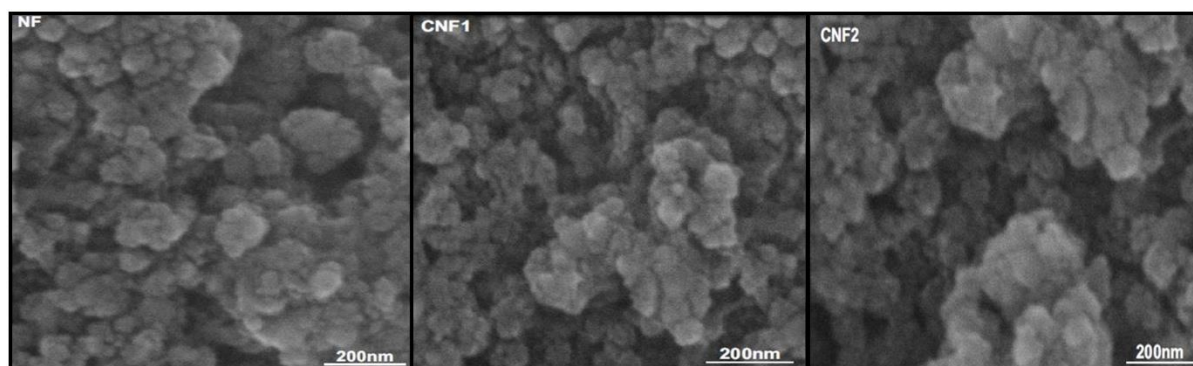


Fig. 3 SEM images for NF, CNF1 and CNF2

VSM analysis

VSM (vibrating sample magnetometer) ranging from -8Koe to +8Koe at 300k was used to determine the magnetic properties of the prepared samples. The M-H curves for NF, CNF1 and CNF2 are shown in figure 4. The magnetic properties comprise magnetization saturation (M_s), remnant magnetization (M_r) and coercivity (H_c) that can be studied in detail from the M-H curve. The magnetic properties of the formed NPs are basically dependent on various

parameters such as distribution of the cations among tetra and octahedral sites, size of the formed crystal and composition etc. [36], the other factors might be spinning canting effect, presence of glass like surface layer above the formed NPs [3, 34,37].

The magnetization saturation values for samples NF, CNF1 and CNF2 were recorded as 29.6 emu/g, 30.2 emu/g and 37.8 emu/g respectively. Which is quite smaller than the magnetization saturation of the bulk Ni ferrites and Co ferrites which is recorded as 55 emu/g and 1440 emu/g respectively. This change occurs due to the cation distribution at nanoscale [38]. A smaller M_s Value is observed for NF indicating paramagnetic behavior (soft magnet), the M_s Increases to a noticeable degree as the Co is doped in sample CNF1 and CNF2 hence, becoming ferromagnetic material, and the smaller magnitude of M_s is related with the smaller size of the particle. Furthermore, as the magnitude of Co doping increases in samples the particle size also increases giving rise to higher magnetization saturation [34, 38]

The value of remnant magnetization (M_r) for the samples was found to be 3.01 emu/g, 4.5 emu/g and 5.7 emu/g. while the coercivity (H_c), the measure of magneto-crystallite anisotropy for the samples was found 116 Oe, 192 Oe and 241 Oe, which was also found to be dependent on the size of the particle. The anisotropy constant K was calculated by using the formula

$$K = M_s \times H_c / 0.96 \quad (7)$$

The value of K for NF was 3214 emu.Oe/g, for CNF1 was 5840 emu.Oe/g and 9410 emu.Oe/g for CNF2 accordingly. The squareness ratio/ magnetic reversal (M_r/M_s) was calculated as 0.10, 0.14 and 0.15 respectively.

Table 4: values of M_s , M_r , H_c , K and M_r/M_s for NF, CNF1 and CNF2

Sample	Saturation magnetization (M_s) emu/g	Remnant magnetization (M_r) emu/g	coercivity (H_c) Oe	Anisotropy constant (K) emu.Oe/g	Magnetic reversal (M_r/M_s)
NF	29.6	3.01	116	3214	0.10
CNF1	30.2	4.5	192	5840	0.14
CNF2	37.8	5.7	241	9410	0.15

From the above results it's concluded that M_r , M_s and H_c are found to increase subsequently with an increase in Co doping. The graphs for CNF1 and CNF2 show larger hysteresis loops as compared to NF, proving its ferromagnetic behavior of the samples. The increase in the above parameters of magnetic properties is due to the redistribution of cations on tetra and octahedral

sites i.e. on site A Ni has 2 unpaired electrons while Co on site B has 3 unpaired electrons, with an increase in Co the increase in unpaired electrons is given rise that causes increase in saturation magnetization [20, 34, 39]. The other contributing factor is the migration of Fe ions from site A to B when doped with Co, hence giving rise to an increased magnetic moment at site B. [1]

An apparent increase is also noticed in the value of coercivity this is because of the high magneto-crystalline property and spin orbital coupling, as per increase in the amount of Co the magneto crystalline anisotropy is also increased, hence giving rise to increased H_c value [38-39]

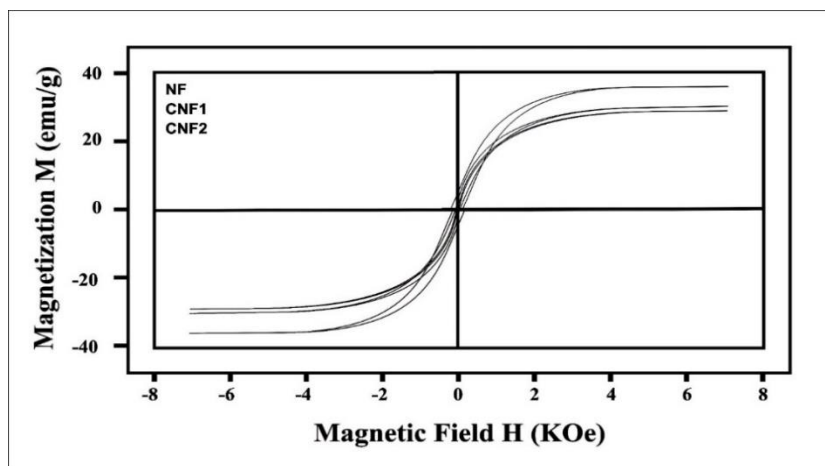


Fig. 4 M-H curves for NF, CNF1 and CNF2

FTIR Analysis

FTIR was performed for the capping agent and one of the samples i.e. NF. It determined the presence of phenolic contents from the extract of the plant onto the formed NPs and the vibrational modes at tetra and octahedral sites. It also confirms the spinel form of the MNPs. To determine the functional group of the extract present on the NPs and its spinel structure, the characterization was performed between the ranges of 400 cm^{-1} to 4000 cm^{-1} . The peaks obtained for various vibrational modes are shown in figure 5. The intensive peak i.e. from 3382 cm^{-1} to less intensive peak 1625 cm^{-1} indicates the O-H stretching vibration of the hydroxyl group, i.e. (-OH), this hydroxyl group indicates the presence of phenolic agent onto the formed NPs that acted as fuel during the formation of NPs [40]. In this region the descending peaks exhibit stretching form of carboxyl group i.e. C=C and C=O indicating the stretching form of the adsorbing water onto the phenols. The next peak at 1346 cm^{-1} exhibits the OH deformation in the phenols [41]. Two crucial bands are observed in the fingerprint region (less than 1000 cm^{-1}) i.e. the higher wave number $\nu_1\ 595\text{ cm}^{-1}$ is produced due to the stretching vibrations of

metal-oxygen i.e (Fe-O) at tetra hedral sites and the lower wave number ν_2 range i.e. 455 cm^{-1} metal oxygen bond of (Ni-O) or ($\text{Co}^{+2}\text{-O}$) stretching vibrations at octahedral sites.

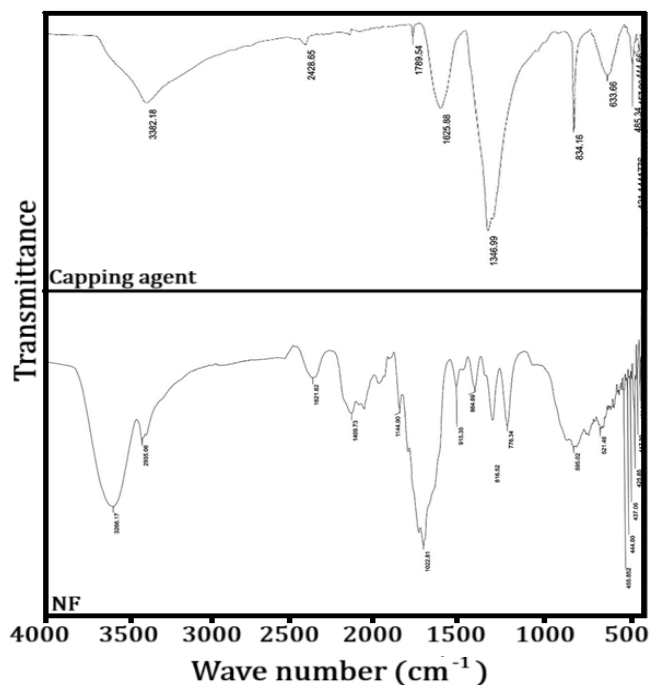


Fig. 5 FTIR spectrum of capping agent and NF

UV-vis Analysis

This analysis is an efficient method to find out the energy band gap of the synthesized NPs. The absorption ranges for NF, NF1 and NF2 are recorded as 306 nm, 302 nm and 300 nm shown in figure 6. This characterization was performed between 200 to 800 nm. The band gap between both direct and indirect for the formed NPs is measured by Tauc’s relation

$$(\alpha \cdot hv)^{1/n} = A(hv - E_g) \dots \dots \dots \text{for indirect energy band gap} \quad (8)$$

$$(\alpha \cdot hv)^n = A(hv - E_g) \dots \dots \dots \text{for direct energy band gap} \quad (9)$$

Where α is the absorption co-efficient, h is the Plank’s constant, ν is the frequency of incident photon, A is another constant, n is the factor, and is 2 for direct energy band gap and $1/2$ for indirect energy band gap [42]. And hv is incident photon energy related to the λ by relation

$$hv = 1240/\lambda \text{ eV} \quad (10)$$

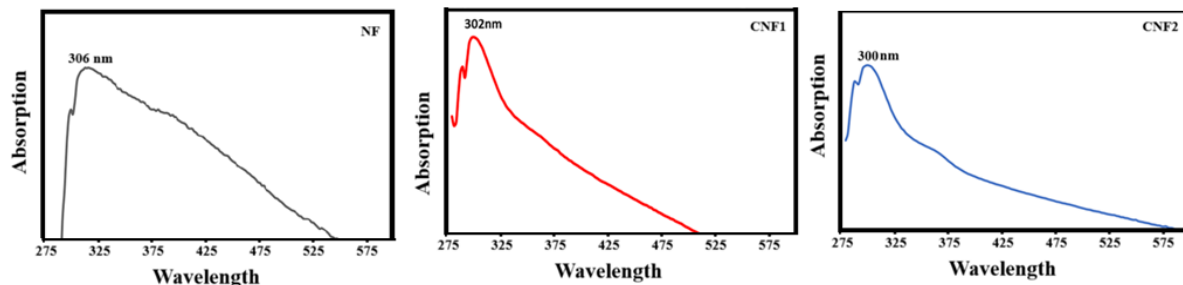


Fig. 6 absorption spectrum of NF, CNF1 and CNF2

The Tauc's plot is shown in figure 7. Where the linear part on x-axis ($\alpha \cdot hv$) = 0, and the tangent line that intercepts on x-axis, denotes the energy band gaps, were found to be 2.92 eV for NF, 3.48 eV for CNF1 and 3.4 eV for CNF2 respectively. In this study the energy band gap for NF is recorded lesser than the cobalt doped nickle ferrites which is not in consistent with other studies, where the energy band gaps for the pure NF has been recorded larger, the reasons for this might be the oxygen vacancies or metal cation occupied spaces, or might be due to stoichiometric ratio deviation of Ni and Fe that can cause alteration in electronic states near Fermi level, hence reducing the actual band gap. The other reason could be quantum confinement effects, and the smaller size of particles that possess larger surface area to volume ratios where the energy levels become discrete causing a shift in absorption spectra, hence resulting in decreased band gap. But the results of CNF1 and CNF2 are found consistent with other studies as the energy band gaps are found to decrease from 3.48 eV to 3.8 eV for CNF1 and CNF2, concluding that with an increase in cobalt dopant a decrease in energy band gap is seen. From the above results it's clear that the band gap is also dependent upon the size of the particle, the larger particle size possesses smaller band gap and vice versa [43] the other contributing factors for the change in energy band gaps are quantum local effect, change in lattice constant, phase purity and concentration of charge carriers [44].

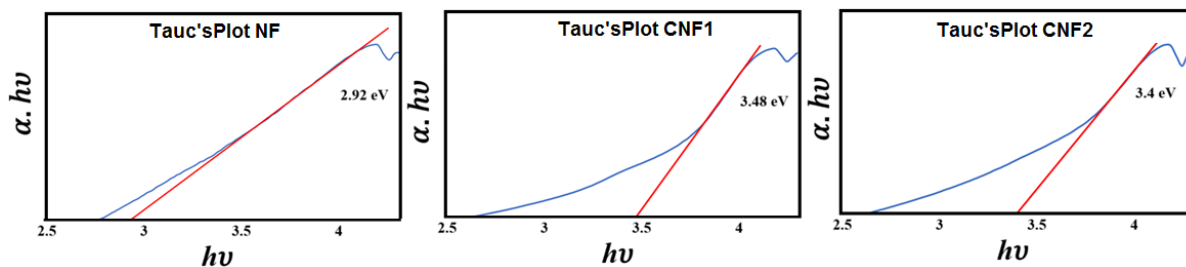


Fig. 7 Tauc's plot for NF, CNF1, CNF2

Conclusions

Ni and Co doped nickle ferrites were prepared via green route using the extract of vitis vinifera which has not been used prior to this work. The green synthesis method was an easy, efficient, environmentally friendly, and less expensive method. 3 samples were prepared named NF, CNF1 and CNF2 and the impact of Co doping on nickel ferrites was studied in detail. The effects of Co doping were confirmed by the characterization tools: XRD confirmed the crystalline and the spinel structure of the formed ferrites, the average crystallite size was found to increase with Co doping and were recorded as 16.8 nm, 17.5 nm and 18.9 nm. The vibrational modes and presence of phenolic contents were analyzed through FTIR. EDX showed the elemental composition of the formed ferrites. VSM revealed that the magnetic properties such

as M_s , M_r and H_c are enhanced with Co doping. Whereas the energy band gap for NF was recorded as 2.92 eV, 3.48 eV for CNF1 and 3.4 eV for CNF2, which indicated the decrease in band gap with an increase in cobalt concentration. The structure and particles size were analyzed via SEM, the average particle sizes were found to increase with Co doping from 46 nm to 57 nm and to 68 nm accordingly.

Acknowledgements

The authors are thankful to the Petroleum Engineering department BUIITEMS, Quetta for providing x-ray diffraction analysis facility, Department of Physics, University of Balochistan for providing UV vis facility, Lahore University of Management Sciences for providing FE-SEM, EDX and VSM facilities and Husein Ebrahim Jamal Research Institute of Chemistry (HEJ) for providing FTIR facility. This research work was funded partly by the Higher Education commission of Pakistan through National Research Project Fund for Universities # 17152.

References

- [1] Chakrabarty, S., Dutta, A., & Pal, M. (2015). Enhanced magnetic properties of doped cobalt ferrite nanoparticles by virtue of cation distribution. *Journal of Alloys and Compounds*, 625, 216-223
- [2] Debnath, S., Das, A., & Das, R. (2021). Effect of cobalt doping on structural parameters, cation distribution and magnetic properties of nickel ferrite nanocrystals. *Ceramics International*, 47(12), 16467-16482.
- [3] Bilal, A., Kasi, J. K., Kasi, A. K., Bokhari, M., Ahmed, S., & Ali, S. W. (2022). Environment friendly synthesis of nickel ferrite nanoparticles using *Brassica oleracea* var. capitata (green cabbage) as a fuel and their structural and magnetic characterizations. *Materials Chemistry and Physics*, 290, 126483.
- [4] Ibrahim, I. D., Jamiru, T., Sadiku, E. R., Hamam, Y., Alayli, Y., & Eze, A. A. (2019). Application of nanoparticles and composite materials for energy generation and storage. *IET Nanodielectrics*, 2(4), 115-122.
- [5] Alijani, H. Q., Pourseyedi, S., Torkzadeh-Mahani, M., Seifalian, A., & Khatami, M. (2020). Bimetallic nickel-ferrite nanorod particles: greener synthesis using rosemary and its biomedical efficiency. *Artificial cells, nanomedicine, and biotechnology*, 48(1), 242-251.

- [6] Tatarchuk, T., Liaskovska, M., Kotsyubynsky, V., & Bououdina, M. (2018). Green synthesis of cobalt ferrite nanoparticles using *Cydonia oblonga* extract: structural and mössbauer studies. *Molecular Crystals and Liquid Crystals*, 672(1), 54-66.
- [7] Laokul, P., Amornkitbamrung, V., Seraphin, S., & Maensiri, S. (2011). Characterization and magnetic properties of nanocrystalline CuFe_2O_4 , NiFe_2O_4 , ZnFe_2O_4 powders prepared by the Aloe vera extract solution. *Current Applied Physics*, 11(1), 101-108.
- [8] Manjunatha, M., Reddy, G. S., Mallikarjunaiah, K. J., Damle, R., & Ramesh, K. P. (2019). Determination of phase composition of cobalt nanoparticles using ^{59}Co internal field nuclear magnetic resonance. *Journal of Superconductivity and Novel Magnetism*, 32, 3201-3209.
- [9] Yadav, R. S., Kuřitka, I., Vilcakova, J., Havlica, J., Masilko, J., Kalina, L., ... & Hajdúchová, M. (2017). Structural, magnetic, dielectric, and electrical properties of NiFe_2O_4 spinel ferrite nanoparticles prepared by honey-mediated sol-gel combustion. *Journal of Physics and Chemistry of Solids*, 107, 150-161.
- [10] Khan, A. A., Javed, M., Khan, A. R., Iqbal, Y., Majeed, A., Hussain, S. Z., & Durrani, S. K. (2017). Influence of preparation method on structural, optical and magnetic properties of nickel ferrite nanoparticles. *Materials Science-Poland*, 35(1), 58-65.
- [11] Almessiere, M. A., Korkmaz, A. D., Slimani, Y., Nawaz, M., Ali, S., & Baykal, A. (2019). Magneto-optical properties of rare earth metals substituted Co-Zn spinel nanoferrites. *Ceramics International*, 45(3), 3449-3458.
- [12] Khoso, W. A., Haleem, N., Baig, M. A., & Jamal, Y. (2021). Synthesis, characterization and heavy metal removal efficiency of nickel ferrite nanoparticles (NFN's). *Scientific Reports*, 11(1), 3790.
- [13] Barkule, R. S., Kurmude, D. V., Raut, A. V., Waghule, N. N., Jadhav, K. M., & Shengule, D. R. (2014). Structural and electrical conductivity studies in nickel ferrite nano-particles. *Solid State Phenomena*, 209, 177-181.
- [14] Paul, C. A., Kumar, E. R., Abd El-Rehim, A. F., & Yang, G. (2023). Cobalt oxide nanoparticles for biological applications: synthesis and physicochemical characteristics for different natural fuels. *Ceramics International*, 49(24), 40244-40257.
- [15] Ozcelik, B. E. K. İ. R., Ozçelik, S., Amaveda, H., Santos, H., Borrell, C., Saez-Puche, R., ... & Angurel, L. (2020). High speed processing of NiFe_2O_4 spinel using a laser furnace. *Journal of Materiomics*, 6(4).

- [16] Gayathri Manju, B., & Raji, P. (2020). Green synthesis, characterization, and antibacterial activity of lime-juice-mediated copper–nickel mixed ferrite nanoparticles. *Applied Physics A*, 126(3), 156.
- [17] Baykala, A., Eryiğit, Ş., Amir, M., Güngüneş, H., Sözeri, H., Shirsath, S. E., ... & Asiri, S. M. (2017). Magnetic properties and cation distribution of bimetallic (Mn–Co) doped NiFe₂O₄ nanoparticles. *Journal of Inorganic and Organometallic Polymers and Materials*, 27, 1893-1900.
- [18] Jadhav, P., Patankar, K., Mathe, V., Tarwal, N. L., Jang, J. H., & Puri, V. (2015). Structural and magnetic properties of Ni_{0.8}Co_{0.2-2x}Cu_xMn_xFe₂O₄ spinel ferrites prepared via solution combustion route. *Journal of Magnetism and Magnetic Materials*, 385, 160-165.
- [19] Khanvilkar, M. B., Nikumbh, A. K., Pawar, R. A., Karale, N. J., Nagwade, P. A., Nighot, D. V., ... & Panchgalle, S. P. (2023). Effect of divalent/trivalent doping on structural, electrical and magnetic properties of spinel ferrite nanoparticles. *Engineered Science*, 22(3), 850.
- [20] Kambale, R. C., Shaikh, P. A., Kamble, S. S., & Kolekar, Y. D. (2009). Effect of cobalt substitution on structural, magnetic and electric properties of nickel ferrite. *Journal of Alloys and Compounds*, 478(1-2), 599-603.
- [21] Sundram, S., Baskar, S., & Subramanian, A. (2022). Green synthesized nickel doped cobalt ferrite nanoparticles exhibit antibacterial activity and induce reactive oxygen species mediated apoptosis in MCF-7 breast cancer cells through inhibition of PI3K/Akt/mTOR pathway. *Environmental Toxicology*, 37(12), 2877-2888.
- [22] Ati, M. A., Khudhair, H., Dabagh, S., Rosnan, R., & Ati, A. A. (2014). Synthesis and characterization of cobalt doped nickel-ferrites nanocrystalline by co-precipitation method. *International Journal of Scientific & Engineering Research*, 9(9), 927-930.
- [23] Kadam, A. A., Shinde, S. S., Yadav, S. P., Patil, P. S., Rajpure, K. Y. (2013). Structural, morphological, electrical and magnetic properties of Dy doped Ni–Co substitutional spinel ferrite. *Journal of Magnetism and Magnetic materials*, 329, 59-64.
- [24] Chakradhary, V. K., Ansari, A., & Akhtar, M. J. (2019). Design, synthesis, and testing of high coercivity cobalt doped nickel ferrite nanoparticles for magnetic applications. *Journal of Magnetism and Magnetic Materials*, 469, 674-680.

- [25] Bindu, K., Ajith, K. M., & Nagaraja, H. S. (2019). Influence of cations on the dielectric properties of spinel structured nanoferrites. *Materials Research Express*, 6(4), 045011.K.
- [26] Zhang, Z., Yao, G., Zhang, X., Ma, J., & Lin, H. (2015). Synthesis and characterization of nickel ferrite nanoparticles via planetary ball milling assisted solid-state reaction. *Ceramics International*, 41(3), 4523-4530.
- [27] Ahmed, S., Kasi, J. K., Kasi, A. K., Bokhari, M., Bilal, A., & Ali, S. W. (2023). Phyto-mediated synthesis of enhanced band gap ZnO and TiO₂ nanoparticles using *Pisum sativum* peels extract: comparison of their structural, optical, photocatalytic and antifungal characteristics. *Chemical Papers*, 77(12), 7697-7715
- [28] Kulkarni, G. D., Khedkar, M. V., Somvanshi, S. B., Borade, R. M., More, S. D., & Jadhav, K. M. (2021). Green synthesis and investigations of structural, cation distribution, morphological, and magnetic properties of nanoscale nickel ferrites: the effect of green fuel proportion. *Phase Transitions*, 94(12), 994-1005.
- [29] Karakas, K. Z., Boncukcuoglu, R., Karakas, I. H., & Yilmaz, M. T. (2012). The effect of pH in nickel ferrite nanoparticles synthesis by hydrothermal method (Doctoral dissertation, Sumy State University).
- [30] Dhanda, N., Thakur, P., Kumar, R., Fatima, T., Hameed, S., Slimani, Y., ... & Thakur, A. (2023). Green-synthesis of Ni-Co nanoferrites using aloe vera extract: Structural, optical, magnetic, and antimicrobial studies. *Applied Organometallic Chemistry*, 37(7), e7110.
- [31] Naik, M. M., Naik, H. B., Kottam, N., Vinuth, M., Nagaraju, G., & Prabhakara, M. C. (2019). Multifunctional properties of microwave-assisted bioengineered nickel doped cobalt ferrite nanoparticles. *Journal of Sol-Gel Science and Technology*, 91, 578-595.
- [32] Naseri, M. G., Saion, E. B., Ahangar, H. A., Hashim, M., & Shaari, A. H. (2011). Simple preparation and characterization of nickel ferrite nanocrystals by a thermal treatment method. *Powder Technology*, 212(1), 80-88.
- [33] Sivakumar, P., Ramesh, R., Ramanand, A., Ponnusamy, S., & Muthamizhchelvan, C. (2011). Preparation and properties of nickel ferrite (NiFe₂O₄) nanoparticles via sol-gel auto-combustion method. *Materials Research Bulletin*, 46(12), 2204-2207.
- [34] Debnath, S., & Das, R. (2021). Cobalt doping on nickel ferrite nanocrystals enhances the micro-structural and magnetic properties: Shows a correlation between them. *Journal of Alloys and Compounds*, 852, 156884.

- [35] Ansari, F., Bazarganipour, M., & Salavati-Niasari, M. (2016). NiTiO₃/NiFe₂O₄ nanocomposites: Simple sol–gel auto-combustion synthesis and characterization by utilizing onion extract as a novel fuel and green capping agent. *Materials Science in Semiconductor Processing*, 43, 34-40.
- [36] Majid, F., Dildar, S., Ata, S., Bibi, I., Mohsin, I. U., Ali, A., ... & Ali, M. D. (2021). Cobalt doping of nickel ferrites via sol gel approach: effect of doping on the structural and dielectric properties. *Zeitschrift für Physikalische Chemie*, 235(12), 1811-1829.
- [37] P. Pulišová a,b,n , J. Kováč c , A. Voigt d , P. Raschman, Structure and magnetic properties of Co and Ni nano-ferrites prepared by a twostep direct micro emulsions synthesis,
- [38] Ati, A. A., Othaman, Z., & Samavati, A. (2013). Influence of cobalt on structural and magnetic properties of nickel ferrite nanoparticles. *Journal of Molecular Structure*, 1052, 177-182.
- [39] Kiani, M. N., Butt, M. S., Gul, I. H., Saleem, M., Irfan, M., Baluch, A. H., ... & Raza, M. A. (2023). Synthesis and characterization of cobalt-doped ferrites for biomedical applications. *ACS omega*, 8(4), 3755-3761.
- [40] Maensiri, S., Masingboon, C., Boonchom, B., & Seraphin, S. (2007). A simple route to synthesize nickel ferrite (NiFe₂O₄) nanoparticles using egg white. *Scripta materialia*, 56(9), 797-800.
- [41] Amiri, M., Pardakhti, A., Ahmadi-Zeidabadi, M., Akbari, A., & Salavati-Niasari, M. (2018). Magnetic nickel ferrite nanoparticles: Green synthesis by *Urtica* and therapeutic effect of frequency magnetic field on creating cytotoxic response in neural cell lines. *Colloids and Surfaces B: Biointerfaces*, 172, 244-253.
- [42] Kombaiyah, K., Vijaya, J. J., Kennedy, L. J., & Kaviyarasu, K. (2019). Catalytic studies of NiFe₂O₄ nanoparticles prepared by conventional and microwave combustion method. *Materials Chemistry and Physics*, 221, 11-28.
- [43] Lassoued, A., & Li, J. F. (2020). Magnetic and photocatalytic properties of Ni–Co ferrites. *Solid State Sciences*, 104, 106199.
- [44] Peng, L. P., Fang, L., Yang, X. F., Li, Y. J., Huang, Q. L., Wu, F., & Kong, C. Y. (2009). Effect of annealing temperature on the structure and optical properties of In-doped ZnO thin films. *Journal of Alloys and Compounds*, 484(1-2), 575-579.